Hindawi
Journal of Nanomaterials
Volume 2022, Article ID 8967528, 9 pages
https://doi.org/10.1155/2022/8967528

*Research Article*

# Application of Nanostent Materials Combined with Sports Rehabilitation Therapy in the Treatment of Hip Injury in Outdoor Sports Athletes

**Dan Li**

*College of Physical Education, Xuchang University, Xuchang, 461000 Henan, China*

Correspondence should be addressed to Dan Li; 12003040@xcu.edu.cn

Received 15 March 2022; Revised 26 April 2022; Accepted 7 May 2022; Published 2 June 2022

Academic Editor: Awais Ahmed



With the rapid development of outdoor sports in our country, the condition of hip joint injury of athletes appears constantly. With the continuous progress of modern biotechnology and iatrotechnique, nanomaterials are also gradually used in the treatment of biological medicine. The purpose of this study is to use nanoscaffold materials in combination with athletics rehabilitation therapy to treat and analyze hip injuries in athletes. In this study, 290 patients with hip injuries in our hospital from June to October 2019 were studied. The hip joint injury patients were divided into the control group and the experimental group according to sex and age. The recovery of the hip joint injury in normal condition, the recovery in the pharmacotherapy, and the recovery in the combined therapy with the nanoscaffold material were compared. The function of nanoscaffold materials in experiments can be determined by detecting changes in related indicators in vivo. The results showed that there were 48 cases of ligament injury, accounting for 67.7% of hip joint injury. 22 cases had muscle and tendon injury, and 12 cases had articular cartilage injury and bursa injury. There was no significant difference in red blood cells, lymphocytes, and white blood cells after nanoscaffold material drug delivery therapy, while parathyroid hormone and osteocalcin changed greatly, which indicated that nanoscaffold material carrier therapy could promote the absorption and treatment of drugs in hip joint. Therefore, the research conclusions of this paper is that nanoscaffold material combined with rehabilitation therapy can effectively treat athletes with hip joint injury. It will contribute to the research and practical application of nanomaterials in modern medicine.

## 1. Introduction

*1.1. Background Significance.* Hip joint is the most important joint to support body weight in walking. It is very important for the standing position and movement of the body. However, the pain of hip joint activities will have a serious impact on the movement and function of the lower limbs of patients, especially the quality of life of patients including normal work and research. The incidence of hip joint deformation arthropathy, avascular necrosis of thigh head, hip heteromorphic syndrome, and hip joint pain caused by hip infection are high. In outdoor sports, the hip joint is more prone to injury.

The construction of titanium dioxide nanoscaffold materials not only is similar to the natural roughness of the artificial bone material of the artificial titanium but also has excellent hydrophilicity and greatly improves the cell adhesion and proliferation on the surface. Osteoblast-related cells can promote differentiation, proliferation, and induction. Titanium dioxide nanoscaffold materials have excellent adaptability to current biological fixation and embedding technology. Scanning electron microscopy (SEM) showed that osteoblasts have grown into tubular structures of titanium dioxide nanoscaffold materials that can immobilize bone cells. Microporous structures of specific size titanium dioxide nanopowders effectively reduce adhesion of bacteria

and promote growth and formation of bone tissue. Titanium dioxide nanoscaffold material coating is considered to be an excellent drug carrier because of its high surface area ratio. These excellent characteristics are widely used in biomedical fields.

*1.2. Related Work.* In the study of rehabilitation treatment of hip joint injury, Jana believes that the musculoskeletal model must adapt to the patient's unique geometry to predict the patient's specific hip load. His study compared the accuracy of anisotropic and isotropic scaled musculoskeletal models and hip force prediction from standard patient-specific skeletal geometry standards. His method is to analyze 356 hips of 250 adult pelvic radiographs. He applied three scaling methods: hip spacing anisotropic scale, iliac height, iliac width, lateral and inferior trochanter, isotropic scaling of pelvic width, and isotropic scaling of hip spacing. At the same time, he used the inverse static model to estimate the hip joint force when standing on one leg. The accuracy of his method is not high [1]. The Lopes et al.'s study compared the ROM of the hip joint between male patients with contact ACL injury and noncontact ACL injury. Their method was to compare the ROM of ipsilateral hip joint between 35 male patients with contact ACL injury (contact group) and 45 patients with noncontact ACL injury (noncontact group). In addition, imaging evaluation of the hip joint is also used to assess the presence of cam and clamp deformities. His method is unstable [2]. Morimoto et al.'s study measured the electromyographic activity of piriformis muscle in seven hip joint movements with a filament electrode. His method was to first select 11 healthy men without severe low back pain or lower limb injury. A filament electrode was inserted into piriformis muscle, and the surface electrode was attached to the hip muscle and the dominant brachial trunk muscle. Then, the EMG signal amplitudes of 7 kinds of hip joint movements were measured: hip neutral lateral supine abduction, hip neutral lateral supine abduction, hip joint internal rotation lateral supine abduction, hip joint external rotation prone extension, hip joint external rotation prone external rotation, hip joint pronation prone external rotation, and hip joint supine extension. They used repeated measurements of one-way ANOVA to examine the EMG of each of the seven hip movements. Their method is not practical [3].

*1.3. Work of This Paper.* In this paper, the structure of carbon nanoscaffold materials and the classification by layer number, chirality, and morphology are introduced. Then, the mechanical, electrical, and thermal properties of carbon nanoscaffold materials are described in detail. This study also describes hip injury and BASRI-hip score and gives examples of common sports injuries and events. This study describes the characteristics of hip joint movement of sports athletes. In this study, 298 patients in our hospital were divided into different groups according to age and gender. The experimental group was given drug therapy and nanoscaffold material combined rehabilitation therapy, respectively, and the control group was compared with the normal treatment. Observe the changes of blood indexes in the injured part of hip joint and the change of self-state to judge the therapeutic effect. According to the results, the therapeutic effects of hip patients of different genders are different. From the analysis of the treatment of hip joint injury with nanoscaffold material drug loading, the hip joint injury and the type and frequency of injury tissue structure are different in different age groups. The nanoscaffold material combination therapy in this study is very effective in the treatment of hip joint injury.

## 2. Carbon Nanoscaffold Materials and Hip Joint Injury of Sports Athletes

*2.1. Structure of Carbon Nanoscaffold Materials.* Carbon nanoscaffold materials (CNTs) are seamless tubular structures formed by single or multilayer graphite sheets wound around the same axis. The tube wall is a cylindrical surface composed of carbon atoms produced by SP2 hybridization and a hexagonal grid formed by three carbon atoms around it. The two ends are hemispherical rich rings composed of five rings and seven rings. This is formed by the coverage of lean molecules [4, 5]. It can be seen that the structure of carbon nanoscaffold material is a slightly complex one-axis multilayer structure. Carbon nanoscaffold materials (CNTs) are standard one-dimensional carbon nanomaterials because of their nanosized radial size and microscale axial size, showing a very large aspect ratio. In order to better understand the structure of carbon nanoscaffold materials, the academic community mainly uses the following three methods to classify carbon nanoscaffold materials.

*2.1.1. Classification by Layers.* Depending on the number of layers, the carbon nanoscaffold materials are divided into single and multilayer. The smaller the diameter of multiwalled carbon nanoscaffold materials, the larger the spacing between layers. The smaller the diameter, the larger the radius of curvature, the greater the spacing between layers, and the van der Waals force between layers [6, 7].

*2.1.2. Classification by Chirality.* The single-layer carbon nanoscaffold materials can be considered to be formed by curling the graphite sheet with hexagonal network structure [8, 9]. The graphite sheet structure is shown in Figure 1. Among them, $a_1$ and $a_2$ are the unit vectors of the 6-ring lattice with an included angle of 60°. In the figure, select point $O$ as the origin and point OA as toward point $A$. This vector is the chiral vector of carbon nanoscaffold materials as shown below. Through point $O$, create the vertical vector ob of vector OA. This vector is the translation vector of carbon nanoscaffold materials as $t$. Through point $B$, the vector $BB'$ is parallel to the vector OA. Secondly, OABB is the original unit of carbon nanoscaffold materials. The angle between vector OA and vector OD is the rotation angle, and the range is $0° \le |\theta| \le 30°$. The structure of SWCNTs can be expressed by chiral vector $C_h$

$$C_h = na_1 + ma_2 = (n, m). \quad (1)$$

$n, m$ is an integer and $0 \le |m| \le n$. The rotation angle $\theta$ can be expressed by $C_h$ and $a_1$

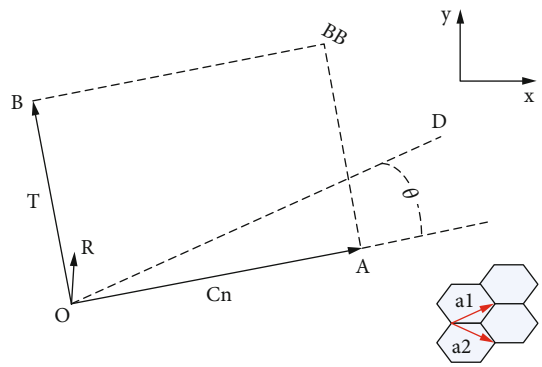


Figure 1: Schematic diagram of carbon nanoscaffold materials formed by graphene sheet.

$$\cos\theta = \frac{C_h a_1}{|C_h||a_1|} = \frac{2n+m}{2\sqrt{n^2+m^2+mn}}. \quad (2)$$

The rotation angle $\theta$ varies with $n, m$. When $\theta = 0^\circ$ and $\theta = 30^\circ$, the CNTs are not helical but chiral. Specific types are divided into armchair type and zigzag type. When $0^\circ \le |\theta| \le 30^\circ$ carbon nanoscaffold materials helix, they show chiral structure [10].

*2.1.3. Classification by Morphology.* According to the various shapes of carbon nanoscaffold materials, in addition to the standard cylindrical shape, carbon nanoscaffold materials can also be divided into L-type, Y-type, or T-type and other different types. These different morphologies of carbon nanoscaffold materials are based on unique topologies. Moreover, there are uncertainties in the preparation process. Now, according to their morphology, carbon nanoscaffold materials can be classified into three types: blocking type, onion type, sea urchin type, variable diameter type, bamboo type, rosary type, spiral type, spindle type, and other abnormal types [11, 12].

*2.2. Properties of Carbon Nanoscaffold Materials*

*2.2.1. Mechanical Properties.* The $SP^2$ hybridization of carbon atoms in carbon nanoscaffold materials makes the strength of carbon nanoscaffold materials very high. In ideal condition, the tensile strength of CNTs is about 800 GPa, and the shear strength is about 500 MPa. In addition, the strength of carbon nanoscaffold materials is about 100 times of steel, about 20 times of carbon fiber, the density of carbon nanoscaffold materials is one sixth of steel, and the weight is half of carbon fiber. The elastic modulus and hardness of carbon nanoscaffold materials are the same as those of diamond, and the CNTs have excellent softness and can keep the original shape after twisting, bending, and stretching. Due to the excellent mechanical properties of carbon nanoscaffold materials, it is called "super fiber" in the field of nanomaterials and has a very wide prospect [13, 14].

*2.2.2. Thermal Properties.* Because CNT is large in aspect, heat is transmitted in the axial direction, and the thermal conductivity in the radial direction is average. In this study, 3000 K CNT extends only in the radial direction, and six ring structures remain on the wall of the tube. When the axial size of carbon nanoscaffold materials exceeds 10 nm, the thermal conductivity may reach 6000 W/m·k at room temperature and 280 W/m·k at low temperatures. In certain size ranges, carbon nanoscaffold material length and thermal conductivity are linear functions. Carbon nanoscaffold materials can be used as additives for composite materials and can help improve the thermal conductivity of composite materials [15, 16].

*2.2.3. Electrical Performance.* The electrical properties of carbon nanoscaffold materials are very unique, which may show various conductive properties such as semiconductors and metals. The chiral classification of carbon nanoscaffold materials shows that the rotation angle of carbon nanoscaffold materials is determined by the integers $n$ and $M$. the conductivity of carbon nanoscaffold materials is closely related to the rotation angle. In some studies, armchair carbon nanoscaffold materials exhibit excellent electrical conductivity when $n = M$. In the case of zigzag and chiral carbon nanoscaffold materials, $N - M = 3Q$ ($q$ is an integer) denotes metallicity. When $nm = 3Q$ is not satisfied, the semiconductor property is indicated. The conductivity of carbon nanoscaffold materials is not only related to the size and rotation angle but also vulnerable to the influence of electric and magnetic fields. If the electric and magnetic fields are applied, carbon nanoscaffold materials will change from metal to semiconductor. The good conductivity and curvature radius of carbon nanoscaffold materials are very small, the open electric field is very low, and the field emission characteristics of carbon nanoscaffold materials are very good [17, 18].

*2.3. Hip Joint Injury.* According to the BASRI hip scoring system for ankylosing spondylitis, >12 points were defined as radiation-induced femoral joint lesions. On the images, there are subchondral bone marrow edema, synovial fluid, abnormal synovial enhancement, or arthritis, which are considered to be signs of active inflammatory changes. Moreover, subchondral erosive destruction, articular cavity stenosis, sclerosis, and stiffness are considered to be the results of chronic inflammatory changes. Body fluid was defined as sufficient fluid around the neck of the leg or the inflated femoral joint capsule on T2 or stir images. Symptomatic femoral joint disease is defined as present or past pain or limitation of femoral joint motion [19, 20].

The hip joint with an abnormal X-ray was given a score of 1. The score of 0 indicates that the hip joint is normal; the score of 1 indicates that the hip joint may be abnormal; the score of 2 indicates that the hip joint is mildly abnormal and the joint space is narrowed significantly; the score of 3 indicates moderate abnormalities in the hip joint, and the joint space is >2 mm; the score of 4 indicates severe abnormalities in the hip joint, the bones have been deformed, and the contact range between the articular surfaces of the bilateral bones is >2 cm.

*2.4. Common Sports Injuries and Events.* The following are the common sports injuries and events:

(1) Femoral head fracture: most of the complications of hip joint dislocation and easy injury items are white driving and car racing [21].

(2) Femoral neck fracture: the fracture of adduction or abduction is caused by osteoporosis and falling down, which is easy to be injured in the elderly who participate in sports.

(3) Femoral neck Palau fracture: race class periodic heavy load and easy to hurt events are long-distance runners and recruits.

(4) Hip joint sprain and synovium imbedding: sprained hind leg has "lengthening" phenomenon; you can easily get hurt in gymnastics [22].

(5) Dislocation of hip joint: anterior, posterior, and central dislocation and easy injury items are bicycle and car race [23].

(6) Femur tip slip: Sports injuries due to gymnastics and wrestling can easily lead to disorders of blood supply to the epiphysis.

(7) Osteoarthritis of the femoral head: excessive training in adolescence causes the bone supply disorder of the femoral epiphyseal; fragile events are gymnastics or long distance running.

(8) Hip joint disease: dancing too much can also cause hip injuries.

(9) Contracture and elastic effects of tibial tract: these may be associated with hip injections, and simple injury events are jumping [24].

(10) Iliopsoas key bounce and psoas muscle sliding: it is related to the slight over Zhong or "side leg" exercise, and the vulnerable items are gymnastics and dance.

(11) Bursitis: Gymnastics can also easily lead to iliac hematomas and femoral nerve palsy, hip hyperextension injuries or muscle strains when the buttocks hits the ground.

(12) Intertrochanteric fracture of femur and tendon strain and operation end disease: sprain or hip injury during hurdle and easy injury items are hurdle, gymnastics, and dance.

(13) Trochanteric bursitis of femur: the greater trochanter rubs against the iliotibial tract during running. The vulnerable event is middle and long distance running [25].

*2.5. Hip Joint Movement Characteristics of Sports Athletes.* The special physical characteristics of sports refers to the main physical characteristics shown in mechanics and biology for the purpose of maximizing sports efficiency under the permission of competition rules. In the new gymnastics, mastering the characteristics and training rules of sports is the precondition of physical training. Cognitive characteristic is an important link to improve the level of physical training. Understanding and mastering specific training rules is to improve training efficiency. Maintain the basic conditions of high-quality training for a long time. In the case of new sports, the flexibility of the hip joint can be improved more scientifically by correctly understanding the characteristics of the athletes' hip joint, correctly grasping the strength of the hip joint and understanding the characteristics of the hip joint. The wide movable area of the hip joint is one of the important sports characteristics of the player's hip joint [26, 27].

## 3. Nanoscaffold Material Preparation and Hip Joint Injury Treatment Experiment

*3.1. Data of Experimental Objects.* This data group collected 290 joint fractures and dislocation of sciatic nerve damage in my hospital from June to October 2019. They were 7-59 years old (average $32.83 \pm 10.12$ years). All patients have complete blood circulation, liver function, renal function, coagulation function, erythrocyte sedimentation rate (ESR), C-reactive protein (CRP) and HLA-B27 gene determination, parathyroid hormone (PTH), osteocalcin, 25 hydroxyvitamin D3, end elongation peptide of N type I bone collagen, and B bone, as a result of reren's special placement determination test, Dr or joint CT examination of the pelvis, and iliac MRI results of the joint.

*3.2. Preparation of $TiO_2$ Nanoscaffold Material Cladding Structure.* Pure titanium is used for preheating, after removing the oxide film on the surface, grinding, cleaning, and drying. Electrochemical anodizing establishes an electrochemical anodizing system in which the titanium side is the anode and the platinum side is the anode. In the mixed solution system of the cathode, ammonium fluoride, and ammonium hydrogen phosphate, the oxidation voltage is controlled by a constant 15 V for 60 minutes. Scanning electron microscopy (SEM) confirmed that the coating structure of nanosized $TiO_2$ nanoscaffold material is $TiO_2$ nanoscaffold material. According to the various specifications required in the subsequent experiments, cylindrical titanium dioxide nanoscaffold material-coated titanium rods with a length of 30 mm and a diameter of 3 mm and a thin titanium dioxide nanoplate with a length of 10 mm and a width of 10 mm were fabricated. Put the sample into a steam pressure cooker at 120°C, kill the bacteria for 30 minutes, and then use it after ultrasonic cleaning and drying. Moreover, pure Ti metal samples are cut into the same size for use.

*3.3. Preparation of TiO2 Nanoscaffold Material Coating Loaded with Gentamicin.* A pipette was used to determine the concentration of 1 mg of the prepared intercontinental mycin solution (100 mg/mL), which was added to the prepared $10\,\text{mm} \times 10\,\text{mm}$ $TiO_2$ nanoscaffold material-coated film and then removed. When the negative pressure device is opened in the dark, the suction value of negative pressure gradually rises, and the air pressure in the plastic pipe slowly drops to 0.01 KPa. After about 2 hours, the $TiO_2$ nanoscaffold material sheet was removed, and the surface of the $TiO_2$ nanoscaffold material sheet was cleaned with 20 mL

Table 1: Types of hip joint injury in sports.

| Damage form | Male | | Female | |
|---|---|---|---|---|
| | Number of injured | Proportion | Number of injured | Proportion |
| Muscle and muscle leg injury | 22 | 20.3 | 30 | 48.5 |
| Ligament injury | 48 | 44.5 | 42 | 67.7 |
| Bursa injury | 12 | 11.2 | 28 | 45.1 |
| Bone marrow injury | 2 | 1.8 | 24 | 38.8 |
| Articular cartilage injury | 12 | 11.2 | 4 | 6.6 |
| Nerve injury | 2 | 1.8 | 30 | 48.5 |
| Fracture | 2 | 1.8 | 8 | 12.8 |
| Others | 18 | 16.8 | 0 | 0 |

of 0.01 M phosphoric acid buffer, and the liquid used to detect ultraviolet light was recovered. The drug loading efficiency and mass of $TiO_2$ nanoscaffold materials with negative allergen were calculated according to the change of concentration of kanamycin in the solution. In the above experiments, the concentration of L-arginine solution was increased to 200 mg/mL and 300 mg/mL, and the experiment was continued under the same conditions. In the above experiments, the drug loading rates of $TiO_2$ nanoscaffold materials at various concentrations of rhizomycin were measured and compared.

*3.4. In the Determination of Gentamicin Standard Curve, the Specific Steps Are as Follows:*

(1) Weigh the allergen powder with a precision balance of 10 $\mu$ g, 25 $\mu$ g, 50 $\mu$ g, 100 $\mu$ g, 200 $\mu$ g, 500 $\mu$ g, and 1000 $\mu$ g, respectively, and dissolve them in 10 mL 0.01 M PBS buffer solution. Mix well, and use as standard solution for future use

(2) PBS buffer solution was prepared as blank control

(3) The UV absorption values of different concentrations of gentamycin standard solution were determined by UV spectrophotometer at 320 nm wavelength. The standard curve (UV absorption value and the concentration of gentamycin in the solution) was drawn between the two wavelengths, and the regression equation was established

(4) In the above experiments, 2 mL of intercontinental mycin solution measured in each round was completely vibrated. The ultraviolet absorbance value at 320 nm was measured, and the value was restored to the standard curve and regression equation to obtain the concentration of rhizomycin

## 4. Nanoscaffold Materials Combined with Rehabilitation Therapy for the Treatment of Hip Joint Injuries

*4.1. Type and Frequency of Hip Joint Injury.* According to the second standard of sports medicine, the types of injury are divided into muscle leg injury, joint injury, synovial fluid bag injury, bone injury, bone injury, and nerve injury. The types of hip joint injury tissue structure in sports are shown in Table 1.

According to the classification in Table 1 of the patients with femoral joint injury in our hospital, the histological types of hip joint injury of Chinese sports athletes were analyzed. The investigation shows that 48 of 290 sports athletes suffer from ligament injury, accounting for 67.7% of hip joint injury. 22 cases had muscle and tendon injury, and 12 cases had articular cartilage injury and capsule injury. Ligament injury ranks first in the type of tissue structure of hip joint injury. The main tissue structures of Chinese sports athletes are hip joint injury, ligament injury, muscle and tendon injury, articular cartilage injury, synovial fluid bag injury, and bone end injury. Some athletes were injured on the hip joint at the same time, which was very serious. The season of hip joint injury of athletes is shown in Figure 2.

According to Figure 2, 108 athletes who were injured in the femoral joint of the athletes were classified, and the injury season often occurred in winter and then continued in summer. And the spring and autumn players were injured. The main reasons are low temperature in winter, high muscle viscosity of athletes, poor preparation, and so on. In hot summer, athletes consume a lot of energy and can not supplement energy in time, and concentration force decreases.

*4.2. Therapeutic Effect of Different Gender Hip Joint Patients Based on Nanoscaffold Material Combination Therapy.* To exclude the impact of gender factors on the test results, we compared the differences between the two case groups. The distribution of hemoglobin, red blood cell, and red blood cell and the sedimentation rate of red blood cells were different statistically between men and women. In addition, the special arrangement of Austin starch ($t = 2.06$, $P = 0.041$), $\beta$-bone collagen ($t = 2.073$, $P = 0.040$), and t-pinp ($t = 2.070$, $P = 0.008$) also showed that these bone metabolism indexes were found to be statistically different between the two female groups There are no statistical differences. The experimental test results are shown in Table 2.

As can be seen from Table 2, although the number of cases in this survey is less than that of men, the possibility of hip joint injury is much higher than that of men.

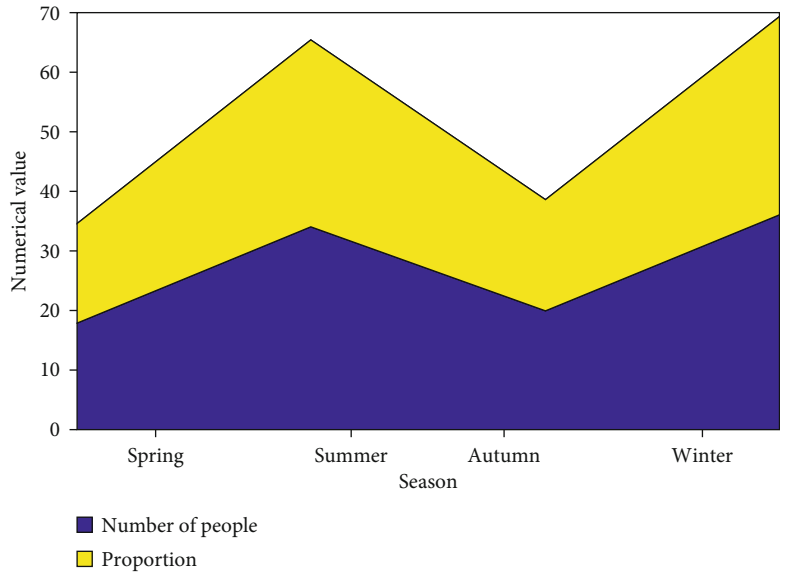


Figure 2: Season of hip joint injury.

Table 2: Experimental results.

| Project | Male | | Female | |
|---|---|---|---|---|
| | Experience group | Control group | Experience group | Control group |
| Number of cases | 67 | 108 | 34 | 24 |
| WBC ($10^9$/L) | 7.14 ± 3.29 | 8.43 ± 8.64 | 8.28 ± 6.52 | 7.36 ± 3.05 |
| LYM ($10^9$/L) | 1.86 ± 0.66 | 1.95 ± 0.63 | 1.88 ± 0.67 | 1.93 ± 0.77 |
| RBC ($10^9$/L) | 4.30 ± 0.62 | 4.52 ± 0.60 | 3.91 ± 0.75 | 4.05 ± 0.41 |
| Hb (g/L) | 116.36 ± 19.22 | 128.37 ± 22.14 | 104.76 ± 15.12 | 113.18 ± 13.31 |
| PTH (pg/mL) | 27.63 ± 12.47 | 30.76 ± 17.77 | 33.64 ± 11.85 | 37.67 ± 25.33 |
| t-PINP (ng/mL) | 84.57 ± 68.48 | 59.98 ± 52.73 | 56.74 ± 74.32 | 42.11 ± 30.07 |
| Osteocalcin (ng/mL) | 29.77 ± 19.25 | 22.54 ± 24.47 | 20.21 ± 15.35 | 20.21 ± 8.61 |

WBC: white blood cell; LYM: lymphocyte; RBC: red blood cell; Hb: hemoglobin; PTH: parathyroid hormone; t-PINP: amino extension end of total type I collagen; osteocalcin: osteocalcin.

The clinical symptoms of hip joint injury are typical groin pain and pain accompanied by dyskinesia of femoral joint. The pain may be caused by acute inflammation and changes of hip joint capsule and synovial nerve. In this study, hip symptoms and image observations were completely inconsistent. This may be related to the following reasons: hip pain and exercise restriction can affect personal subjectivity. The experimental results are shown in Figure 3.

In Figure 3, the number of red blood cells, hemoglobin, and distribution range of red blood cells have a great relationship with femoral joint injury, which can be seen that this is related to hip joint score. The red blood cell distribution width (RDW) and the component of red blood cell routine width reflect the variability of red blood cells in circulation. Traditionally, RDW is a reference index to determine anemia. In many studies, RDW is associated with many diseases, such as polycystic ovary syndrome, coronary artery disease, and heart failure. Inflammation may be the main reason for the relationship between these diseases and RDW, and RDW can be used as an indicator of chronic inflammation.

*4.3. Analysis of Hip Joint Injury in Different Age Groups.* Through the investigation of the injury age of athletes, reflect the characteristics of injury age of athletes. As shown in Figures 4, 290 sports athletes were investigated. In the survey, the main age is 12-17 years and over 50 years, accounting for 34.8% and 37.6% of the players' questionnaire survey, a total of 72.4%. The age distribution of hip joint injury athletes is shown in Figure 4.

As can be seen from Figure 4, women aged 9 to 14 are more injured, while men aged 10 to 16 are more injured. This may be related to the athlete's puberty and joint flexibility. Adolescent athletes are prone to hip injuries due to long-term exercise because their bones are still growing. Over the age of 35, the number of patients with the disease continues to increase with age; both men and women are the same. This is because the physical strength of middle-aged and

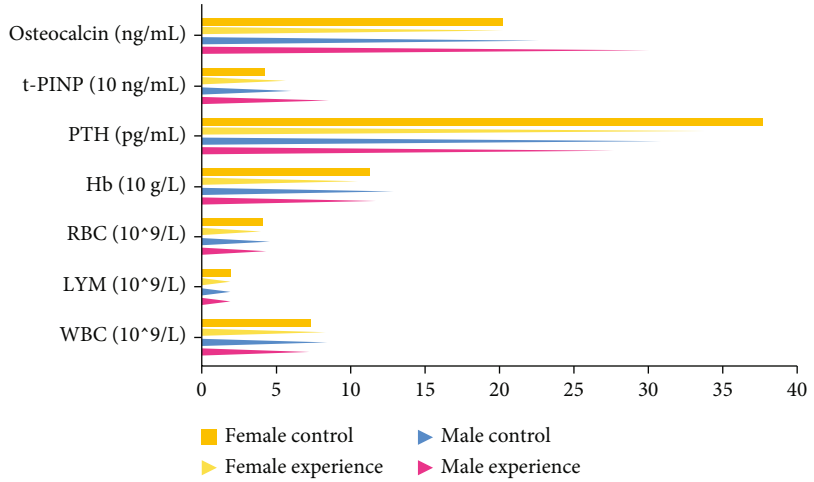


Figure 3: Experimental results.

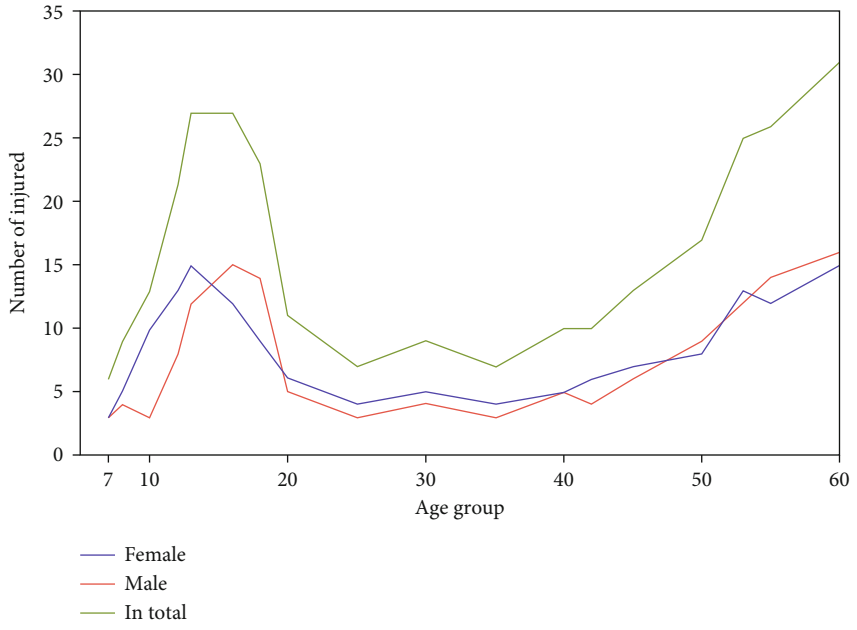


Figure 4: Age distribution of hip injury athletes.

elderly people decreases, the bones gradually relaxed, and a lot of problems are accumulated between joints.

*4.4. Treatment of Hip Joint Injury with Nanoscaffold Material Drug Loading.* Staphylococcus aureus was cultured for 4 hours, and Staphylococcus aureus was observed by a laser scanning confocal microscope on three different materials (pure Ti metal, titanium dioxide nanoscaffold material coating structure material without rhizomycin, and titanium dioxide nanoscaffold material coating structure material containing rhizomycin) on the surface. The colony number and density of Staphylococcus aureus on the surface of pure Ti metal and titanium dioxide nanoscaffold material coating structure material without sulfur group mildew increased significantly. The number of Staphylococcus aureus on the surface of titanium dioxide nanoscaffold material coating structure material was less than that on pure Ti metal surface, but there were still a large number of Staphylococcus aureus appeared throughout the field of vision, but not more, which is obviously concentrated. There was no significant change in the number of Staphylococcus aureus on the surface of titanium dioxide nanoscaffold material coating with rhizomycin compared with that observed in 1 hour. The therapeutic effect of different materials of nanoscaffold material is shown in Figure 5.

It can be seen from Figure 5 that the colonies of Staphylococcus aureus on the surfaces of three different materials (pure Ti free, titanium dioxide nanoscaffold material coating structure material containing past mycin, and titanium dioxide nanoscaffold material coating structure material containing past mycin) after incubation for 1 hour and 4 hours were compared by using image Pro software under a laser

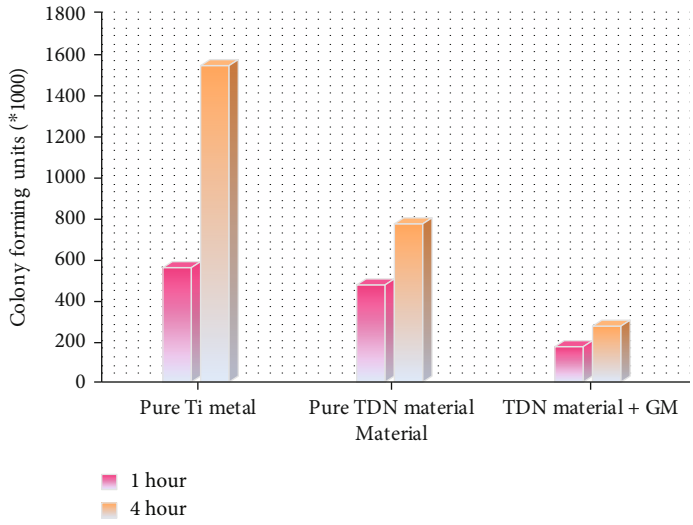


Figure 5: Therapeutic effect of different materials of nanoscaffold materials.

scanning confocal microscope. Regardless of the incubation time of 1 hour or 4 hours, the count of Staphylococcus aureus on the surface of titanium dioxide nanoscaffold materials coated with gentamicin was significantly lower than that of the information group, and the difference was statistically significant ($P < 0.5$). After 1 hour, the amount of S. aureus and S. aureus in the titanium dioxide nanoscaffold material coating material group was less than those on the pure Ti metal surface, but the difference was not statistically significant. After 4 hours of culture, the number of Staphylococcus aureus in the titanium dioxide nanoscaffold material coating structure material group was much lower than that of pure Ti metal surface, and the difference was significant.

## 5. Conclusion

The initial "explosive" release characteristics of TiO2 nanoscaffold material coating with rhizomycin can not play a long-term antibacterial effect in vivo. In animal experiments, Staphylococcus aureus is a common clinical bacterium, which has no obvious effect on the rare fungal infection after artificial joint replacement. In addition, the team has a small number of experimental animals, and the results may be biased. The clinics also have individual differences. Animal experiments alone cannot be extended to clinics. Through the company's internal experiments, it has been confirmed that the titanium dioxide nanoscaffold material coating structure material filled with rhizomycin can effectively inhibit the initial occurrence of infection around the artificial joint after artificial joint replacement, and it has a new therapeutic scheme significance for clinical prevention of infection around artificial joint after artificial joint replacement.

In this study, although there is no significant difference in age and disease course between patients with hip joint injury and those with normal hip joint, according to the Spearman correlation analysis, the degree of hip joint injury is negatively related to the age of onset; that is, the lower the age of onset, the more hip joint occurs. The possibility of damage will increase. There were fewer cases in women than in men in this study, but the probability of hip injury was much higher than in men. The clinical symptoms of hip joint injury are typical inguinal pain and pain accompanied by hip joint dyskinesia. The pain may be caused by acute inflammation or changes in the hip capsule and synovial nerves. This conclusion has great reference significance for promoting the treatment of hip joint injury.

The injury rate of hip joint is 47%, which is the main injury site of Chinese sports athletes. There is a positive correlation between the training years of Chinese sports athletes and the incidence of hip joint injury. Training, talent selection, rules and technology development, nutrition, and other factors are the main causes of hip joint injury of sports athletes. Due to the coach's improper guidance on psychology, cultural quality, flexible sports, clothing, and venue equipment and other factors, it will also have different degrees of impact on sports athletes' hip joint injury. The main effective countermeasures to prevent hip joint injury are to pay attention to scientific and reasonable training methods, strengthen the muscle strength training around the hip joint of athletes, strengthen the standardization of technical sports, do a good job in proper preparatory activities, and establish a scientific Hip protection selection mechanism, improve the public's attention to hip protection, and promote the safety of outdoor sports.

## Data Availability

No data were used to support this study.

## Conflicts of Interest

The authors declare no conflicts of interest.

## References

[1] J. Hornova, V. Kralj-Iglič, D. R. Pedersen, and M. Daniel, "Effect of patient-specific model scaling on hip joint reaction force in one-legged stance – study of 356 hips," *Acta of*

*bioengineering and biomechanics/Wroclaw University of Technology*, vol. 19, no. 4, pp. 103–108, 2017.

[2] O. V. Lopes, J. L. E. Gomes, and D. F. S. Leandro, "Range of motion and radiographic analysis of the hip in patients with contact and non-contact anterior cruciate ligament injury," *Knee Surgery Sports Traumatology Arthroscopy*, vol. 24, no. 9, pp. 2868–2873, 2016.

[3] Y. Morimoto, T. Oshikawa, A. Imai, Y. Okubo, and K. Kaneoka, "Piriformis electromyography activity during prone and side-lying hip joint movement," *Journal of Physical Therapy Science*, vol. 30, no. 1, pp. 154–158, 2018.

[4] S. J. Park, Y. M. Kim, and H. R. Kim, "The effect of hip joint muscle exercise on muscle strength and balance in the knee joint after meniscal injury," *Journal of Physical Therapy ence*, vol. 28, no. 4, pp. 1245–1249, 2016.

[5] D. Rudin, M. Manestar, O. Ullrich, J. Erhardt, and K. Grob, "The anatomical course of the lateral femoral cutaneous nerve with special attention to the anterior approach to the hip joint," *Journal of Bone & Joint Surgery*, vol. 98, no. 7, pp. 561–567, 2016.

[6] M. F. Çatma, S. Ünlü, Ö. Ersan, and A. Öztürk, "Treatment of the bullet, traversing femoral neck, lodged in hip joint: initial arthroscopic removal and subsequent cartilage repair," *Journal of Orthopaedic Case Reports*, vol. 6, no. 4, pp. 13–16, 2016.

[7] M. F. Çatma, A. Öztürk, and M. A. E. Aksekili, "Clinical and functional outcomes of bullet removal from hip joint: five year follow-up of 3 cases," *Duzce Medical Journal*, vol. 6, no. 3, pp. 60–64, 2016.

[8] D. Zhao and H. Xie, "Strategy and discussion of hip joint preserving surgery treatments for adult osteonecrosis of the femoral head," *Chinese Journal of Reparative and Reconstructive Surgery*, vol. 32, no. 7, pp. 792–797, 2018.

[9] Q. Naziri, R. Abraham, J. P. Scollan et al., "Primary total hip arthroplasty for gunshot injury-induced secondary arthritis of the hip: what are the outcomes?," *Journal of Hip Surgery*, vol. 1, no. 4, pp. 200–204, 2018.

[10] T. Yasuda, Y. Yokoi, K. Oyanagi, and K. Hamamoto, "Hip rotation as a risk factor of anterior cruciate ligament injury in female athletes," *Journal of Physical Fitness & Sports Medicine*, vol. 5, no. 1, pp. 105–113, 2016.

[11] Z. Budinski, S. Budinski, M. Vranjes, M. Obradovic, M. Mikic, and M. Milankov, "The relationship between the range of moton of the hip joint with ruptured anterior cruciate ligament," *Medicinski Pregled*, vol. 69, no. 5-6, pp. 160–166, 2016.

[12] H. B. Kak, S. J. Park, and B. J. Park, "The effect of hip abductor exercise on muscle strength and trunk stability after an injury of the lower extremities," *Journal of Physical Therapy ence*, vol. 28, no. 3, pp. 932–935, 2016.

[13] S. Ziying and C. Ping, "Efficacy of bisphosphonates combined with recombinant human parathyroid hormone 1-34 in elderly patients with lumbar or hip joint injury caused by osteoporosis," *Latin American Journal of Pharmacy*, vol. 38, no. 1, pp. 51–56, 2019.

[14] S. Wan, L. Qi, X. Xu, C. Tong, and Z. Gu, "Deep learning models for real-time human activity recognition with smartphones," *Mobile Networks and Applications*, vol. 25, pp. 743–755, 2020.

[15] H. Zhang, C. Song, W. Zhao, A. Yin, J. Zhu, and G. Ren, "Influence of different abduction angles of hip joint on stress distribution of femoral neck," *Shengwu yixue gongchengxue zazhi*, vol. 33, no. 2, pp. 274–278, 2016.

[16] P. Lertwanich, A. Plakseychuk, S. Kramer et al., "Biomechanical evaluation contribution of the acetabular labrum to hip stability," *Knee Surgery, Sports Traumatology, Arthroscopy*, vol. 24, no. 7, pp. 2338–2345, 2016.

[17] A. Babu, A. Gupta, P. Sharma, P. Ranjan, and A. Kumar, "Blunt traumatic superior gluteal artery pseudoaneurysm presenting as gluteal hematoma without bony injury: a rare case report," *Chinese Journal of Traumatology*, vol. 19, no. 4, pp. 244–246, 2016.

[18] M. Yasuhiro, "Gender-related differences in lower limb alignment, range of joint motion, and the incidence of sports injuries in Japanese university athletes," *Journal of Physical Therapy ence*, vol. 29, no. 1, pp. 12–15, 2017.

[19] L. N. Solomin, M. V. Andrianov, M. Takata, and H. Tsuchiya, "Reference positions for transosseous elements in femur: a cadaveric study," *Injury-international Journal of the Care of the Injured*, vol. 47, no. 6, pp. 1196–1201, 2016.

[20] D. V. Kosynkin, A. L. Higginbotham, A. Sinitskii et al., "Longitudinal unzipping of carbon nanotubes to form graphene nanoribbons," *Nature*, vol. 458, no. 7240, pp. 872–876, 2009.

[21] H. Cheng, Y. Zhao, Y. Fan, X. Xie, L. Qu, and G. Shi, "Graphene-quantum-dot assembled Nanotubes: a new platform for efficient Raman enhancement," *ACS Nano*, vol. 6, no. 3, pp. 2237–2244, 2012.

[22] Y. Zhang, Y. Li, and C. Bai, "Microstructure and oxidation behavior of Si-$MoSi_2$ functionally graded coating on Mo substrate," *Ceramics International*, vol. 43, no. 8, pp. 6250–6256, 2017.

[23] B. K. Vijayan, N. M. Dimitrijevic, J. Wu, and K. A. Gray, "The effects of Pt doping on the structure and visible light photoactivity of titania Nanotubes," *Journal of Physical Chemistry C*, vol. 114, no. 49, pp. 21262–21269, 2010.

[24] Y. Zhu, A. Marianov, H. Xu, C. Lang, and Y. Jiang, "Bimetallic Ag-Cu supported on graphitic carbon nitride nano-scaffold materials for improved visible-light photocatalytic hydrogen production," *ACS Applied Materials & Interfaces*, vol. 47, no. 11, pp. 311–318, 2018.

[25] N. Wang, Z. Bai, Y. Qian, and J. Yang, "Double-walled Sb@$TiO_2$−xnanotubes as a superior high-rate and ultralong-lifespan anode material for Na-ion and Li-ion batteries," *Advanced Materials*, vol. 28, no. 21, pp. 4126–4133, 2016.

[26] S. Konduri, H. M. Tong, S. Chempath, and S. Nair, "Water in single-walled aluminosilicate nano-scaffold materials: diffusion and adsorption properties," *The Journal of Physical Chemistry C*, vol. 112, no. 39, pp. 15367–15374, 2008.

[27] R. Leghrib, T. Dufour, F. Demoisson, N. Claessens, F. Reniers, and E. Llobet, "Gas sensing properties of multiwall carbon nanotubes decorated with rhodium nanoparticles," *Sensors & Actuators B Chemical*, vol. 160, no. 1, pp. 974–980, 2011.